Electronic Supplementary Material (ESI) for Inorganic Chemistry Frontiers.


*Supplementary information*

# Two isomeric In(III)-MOFs: Unexpected stability difference and selective fluorescence detection of fluoroquinolone antibiotics in water

Wen-Bin Zhong, Ru-Xia Li, Jie Lv, Tao He, Ming-Ming Xu, Bin Wang, Lin-Hua Xie* and Jian-Rong Li*

Beijing Key Laboratory for Green Catalysis and Separation and Department of Chemistry and Chemical Engineering, College of Environmental and Energy Engineering, Beijing University of Technology, Beijing 100124, P. R. China.

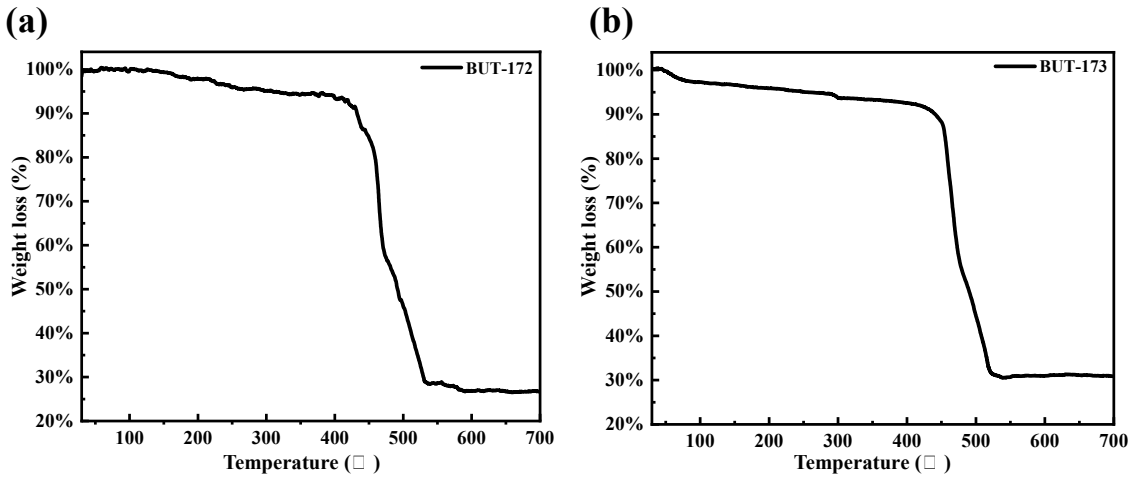


**Fig. S1.** TGA curves of **BUT-172 (a)** and **BUT-173 (b)**.

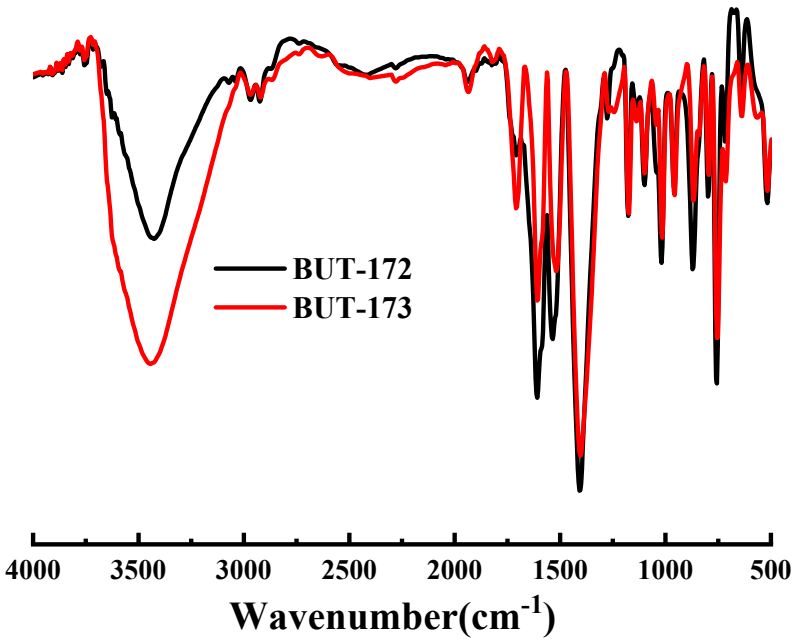


**Fig. S2.** FT-IR spectra of **BUT-172** and **BUT-173**.

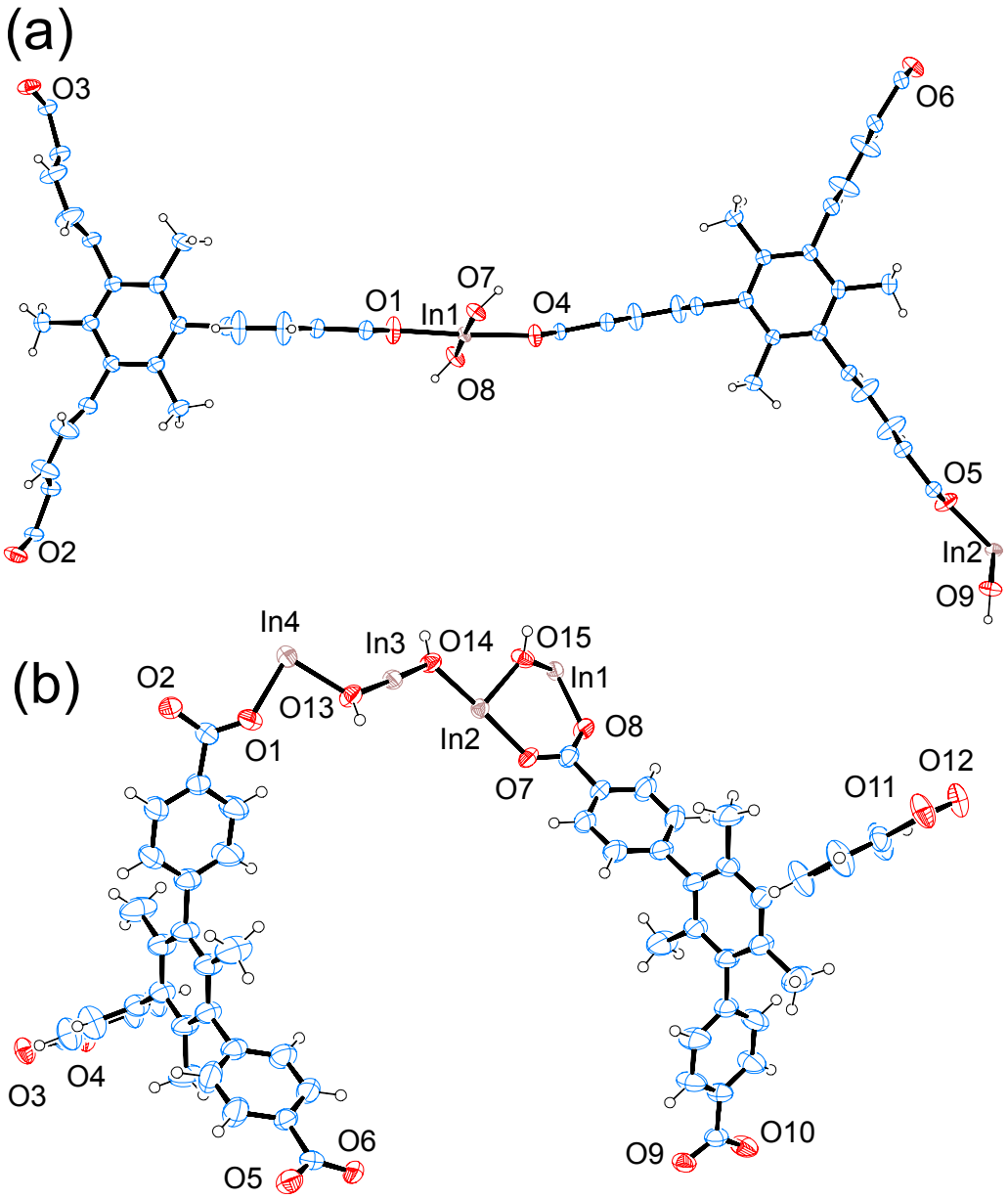


**Fig. S3** An ORTEP view of the asymmetric units of **BUT-172** (a) and **BUT-173** (b). Displacement ellipsoids are represented by 50% probability level.

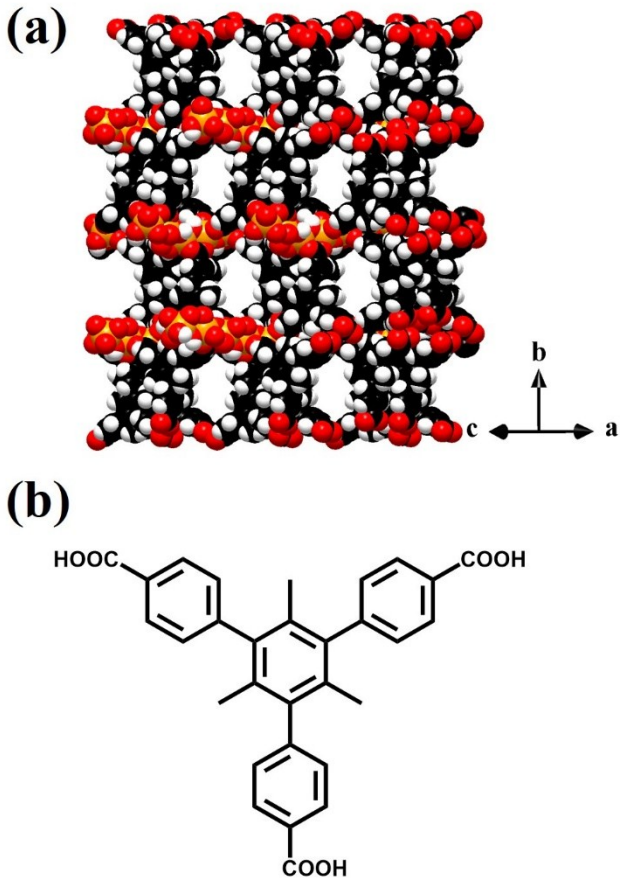


**Fig. S4** (a)The channels in **BUT-173** viewing along the [101] direction, (b) the molecular structure of the $H_3$CTTA ligand.

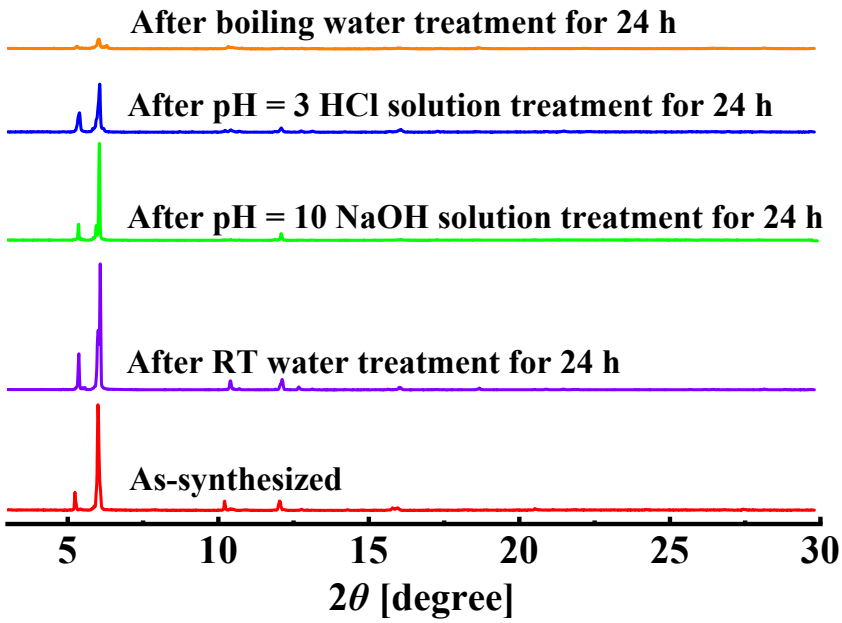


**Fig. S5** PXRD patterns of **BUT-173** before and after stability tests, and PXRD patterns were not normalized to compare their crystallinities.

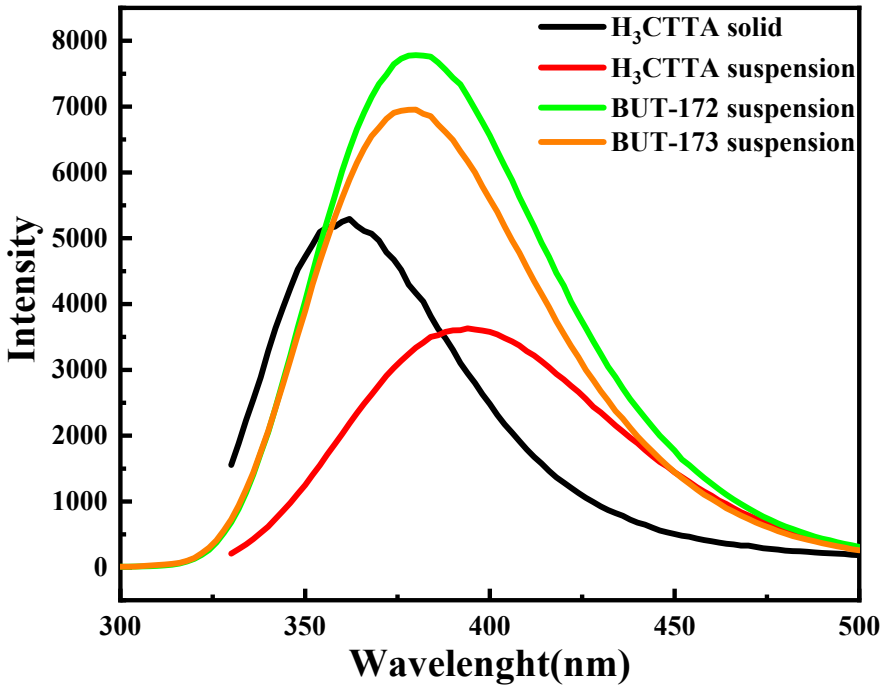


**Fig. S6.** Luminescent spectra of $H_3$CTTA (solid, suspension in water), **BUT-172** and **BUT-173** (suspension in water)

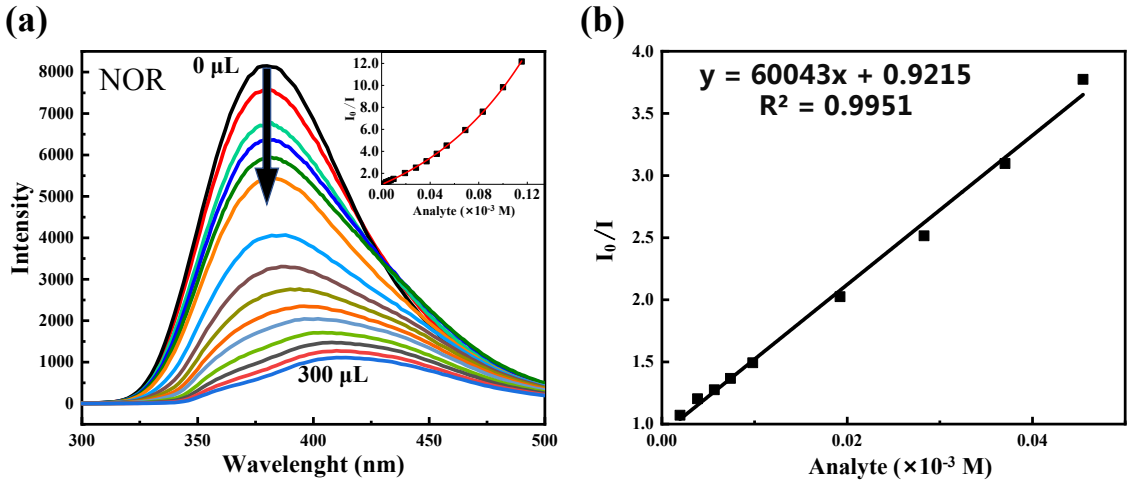


**Fig. S7** (a) Effect on the emission spectra of **BUT-172** dispersed in water upon the incremental addition of 300 µL (500 µM) water solution of NOR, (b) Stern-Volmer plot of NOR.

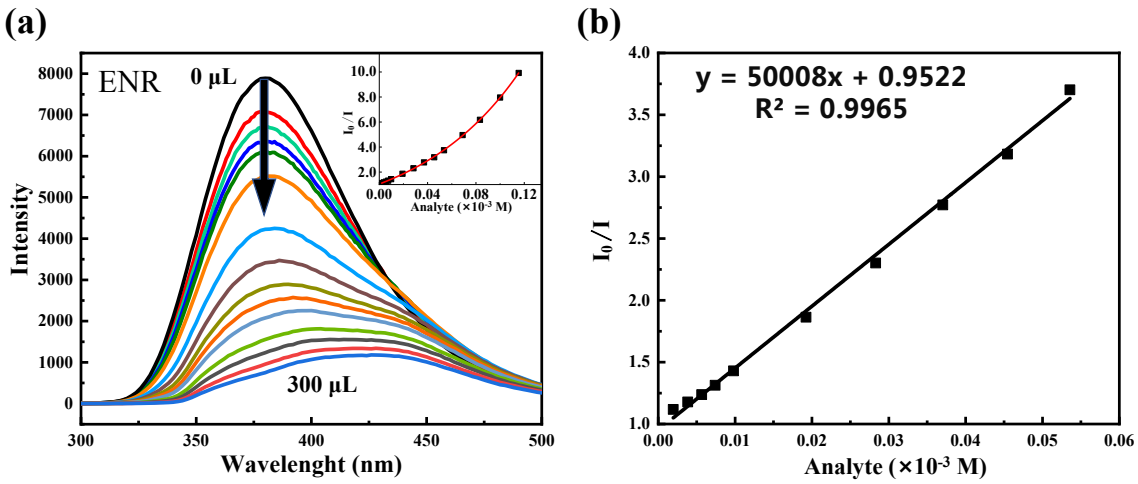


**Fig. S8** (a) Effect on the emission spectra of **BUT-172** dispersed in water upon the incremental addition of 300 µL (500 µM) water solution of ENR, (b) Stern-Volmer plot of ENR.

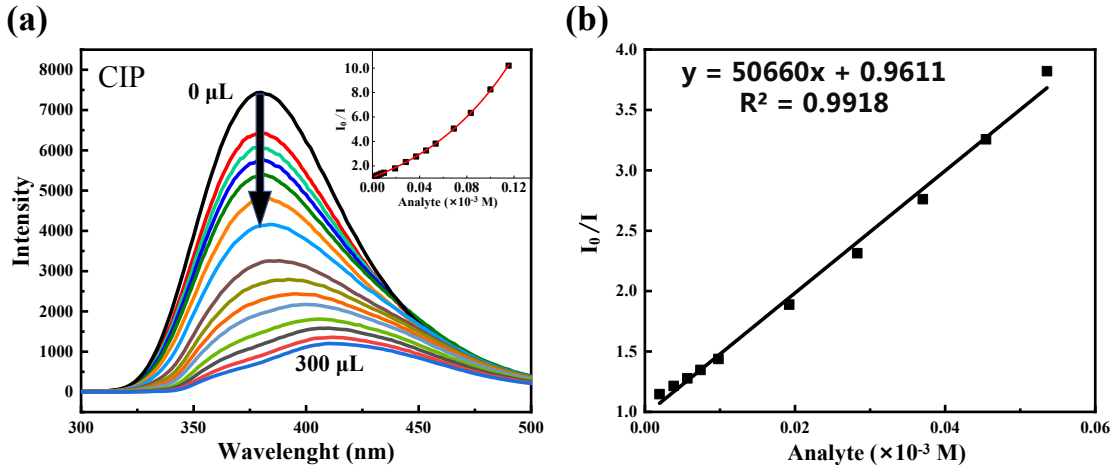


**Fig. S9** (a) Effect on the emission spectra of **BUT-172** dispersed in water upon the incremental addition of 300 µL (500 µM) water solution of CIP, (b) Stern-Volmer plot of CIP.

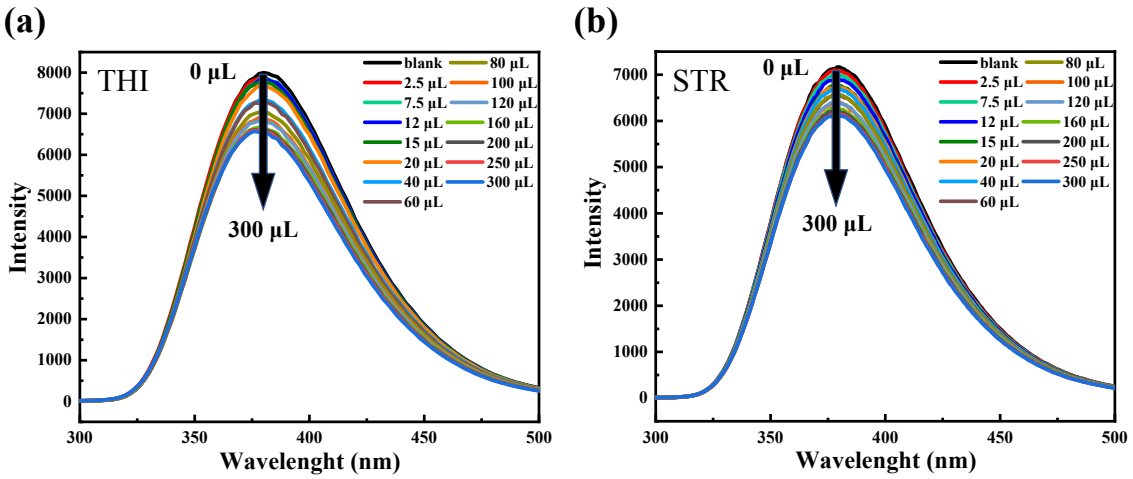


**Fig. S10** Effect on the emission spectra of **BUT-172** dispersed in water upon the incremental addition of 300 µL (500 µM) water solution of (a) THI, (b) STR.

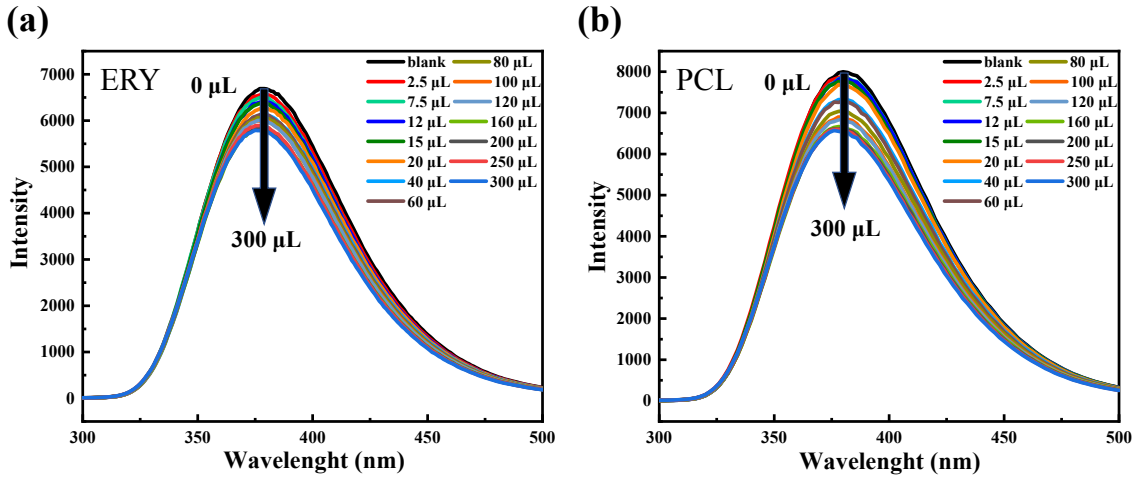


**Fig. S11** Effect on the emission spectra of **BUT-172** dispersed in water upon the incremental addition of 300 µL (500 µM) water solution of (a) ERY, (b) PCL.

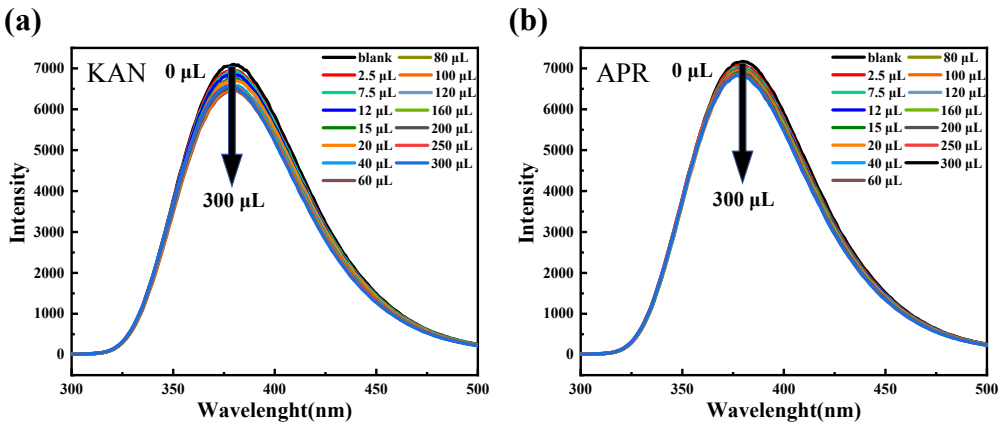


**Fig. S12** Effect on the emission spectra of **BUT-172** dispersed in water upon the incremental addition of 300 μL (500 μM) water solution of (a) KAN, (b) APR.

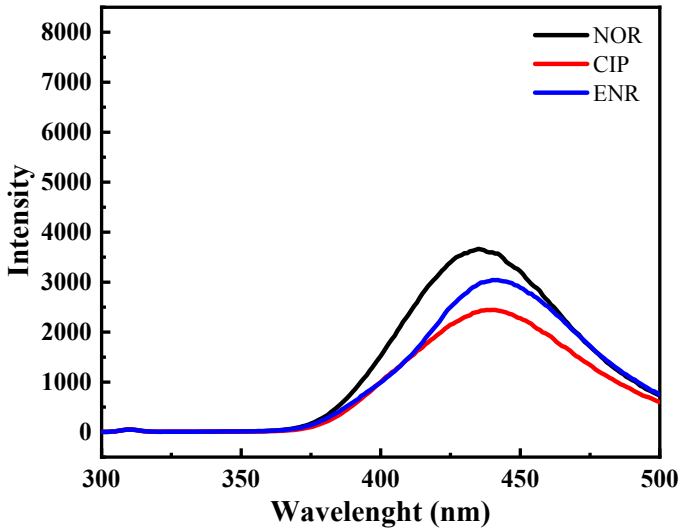


**Fig. S13** The emission spectra of NOR, CIP, ENR (0.11mM) dissolved in water (excitation wavelength 280nm).

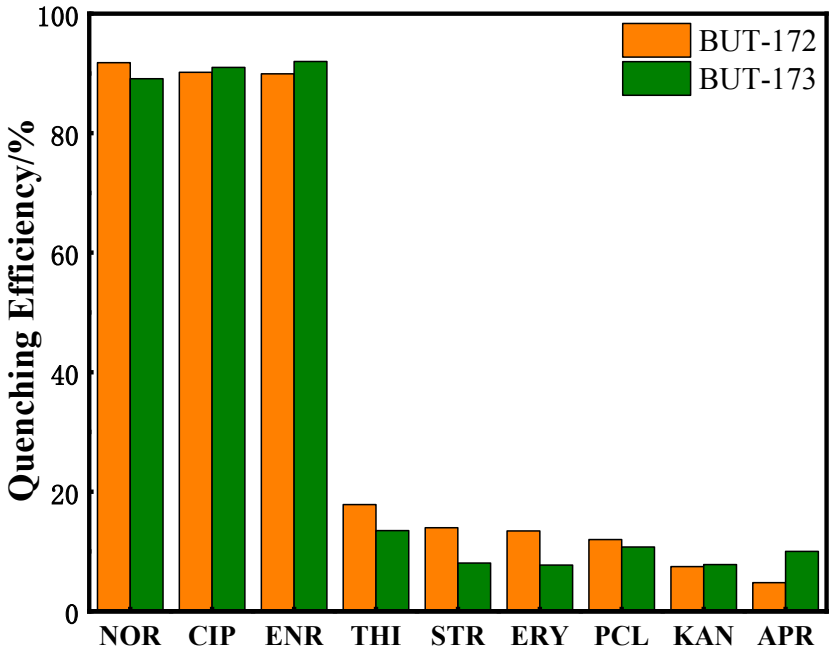


**Fig. S14** Fluorescence quenching efficiencies of **BUT-172** and **BUT-173** by the antibiotics at room temperature.

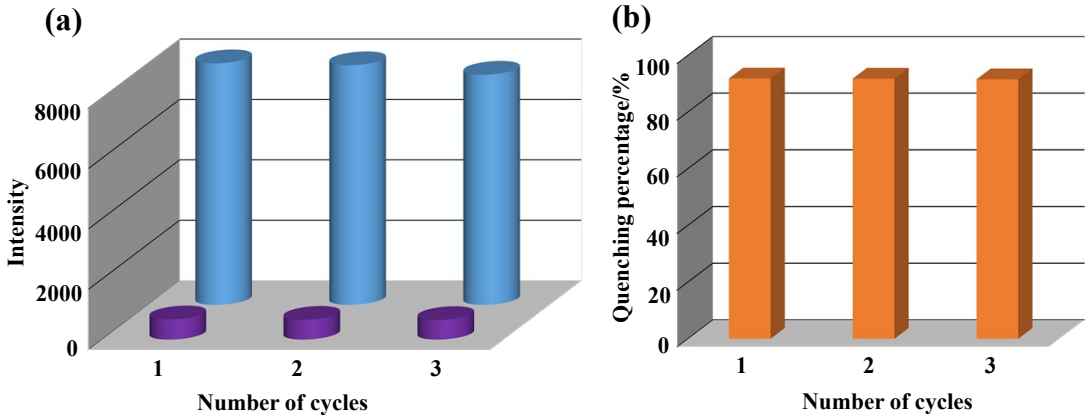


**Fig. S15** (a) The initial fluorescence intensities (blue bars) of the **BUT-172** suspensions and those after the addition of 300 μL NOR (0.5 mM) aqueous solution (purple bars) in each regeneration test. (b) The quenching efficiencies of the **BUT-172** suspensions by the addition of 300 μL NOR (0.5 mM) aqueous solution for each regeneration test.

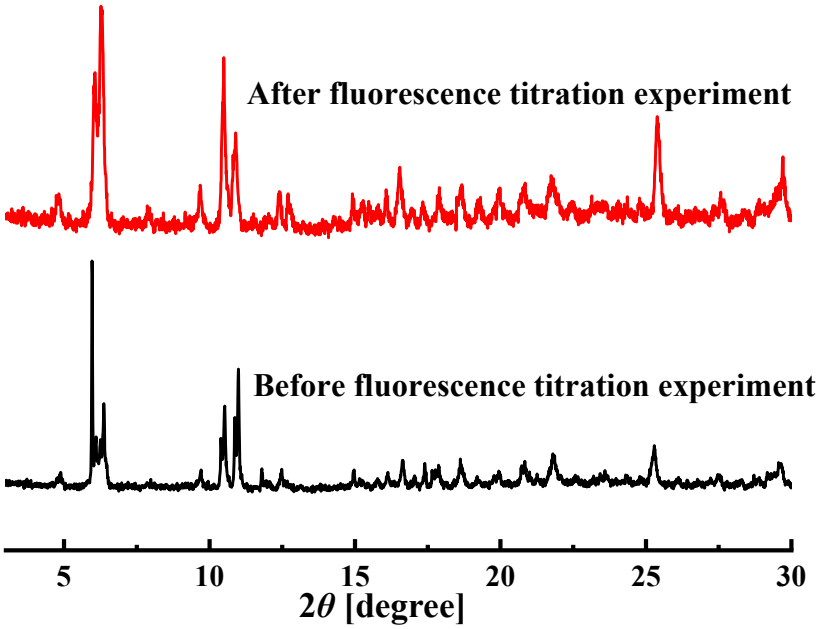


**Fig. S16** The PXRD patterns of **BUT-172** before and after the fluorescence titration experiment.

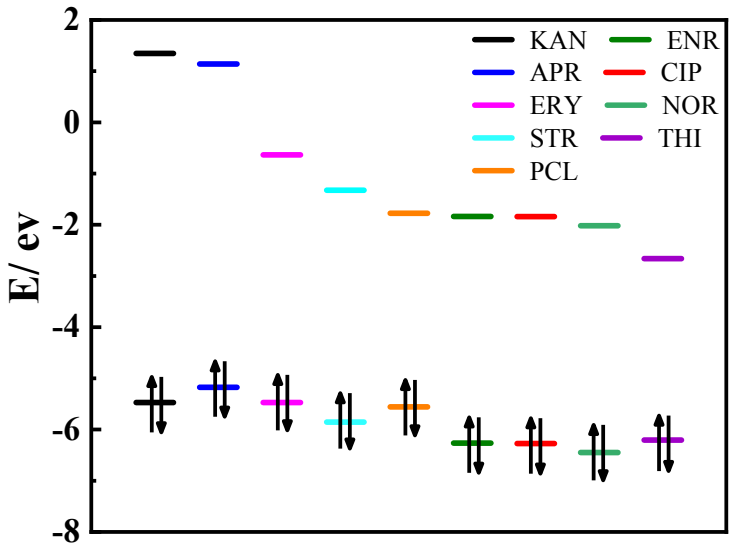


**Fig. S17** HOMO and LUMO energies for selected antibiotics arranged in descending order of LUMO energies.

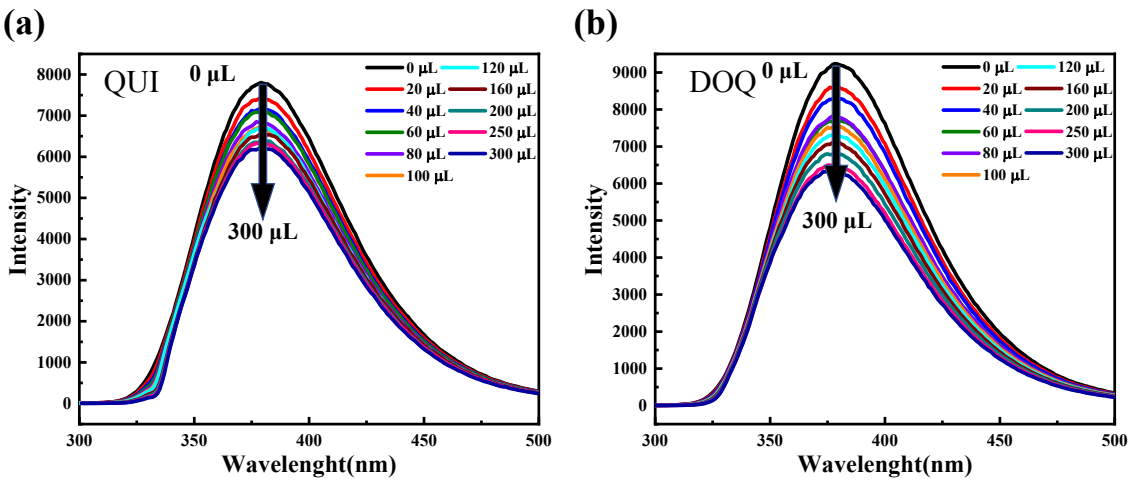


**Fig. S18** The change of the fluorescence of aqueous **BUT-172** suspensions upon the incremental addition of 300 μL aqueous solution of (a) QUI, or (b) DOQ (500 μM).

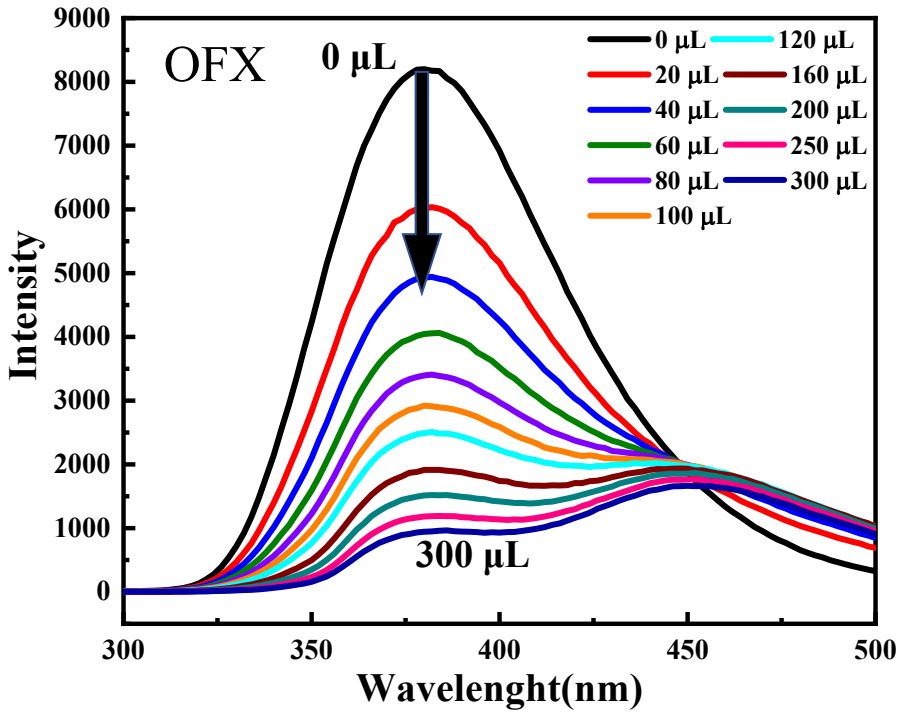


**Fig. S19** The change of the fluorescence of an aqueous **BUT-172** suspension upon the incremental addition of 300 μL aqueous solution of OFX (500 μM).

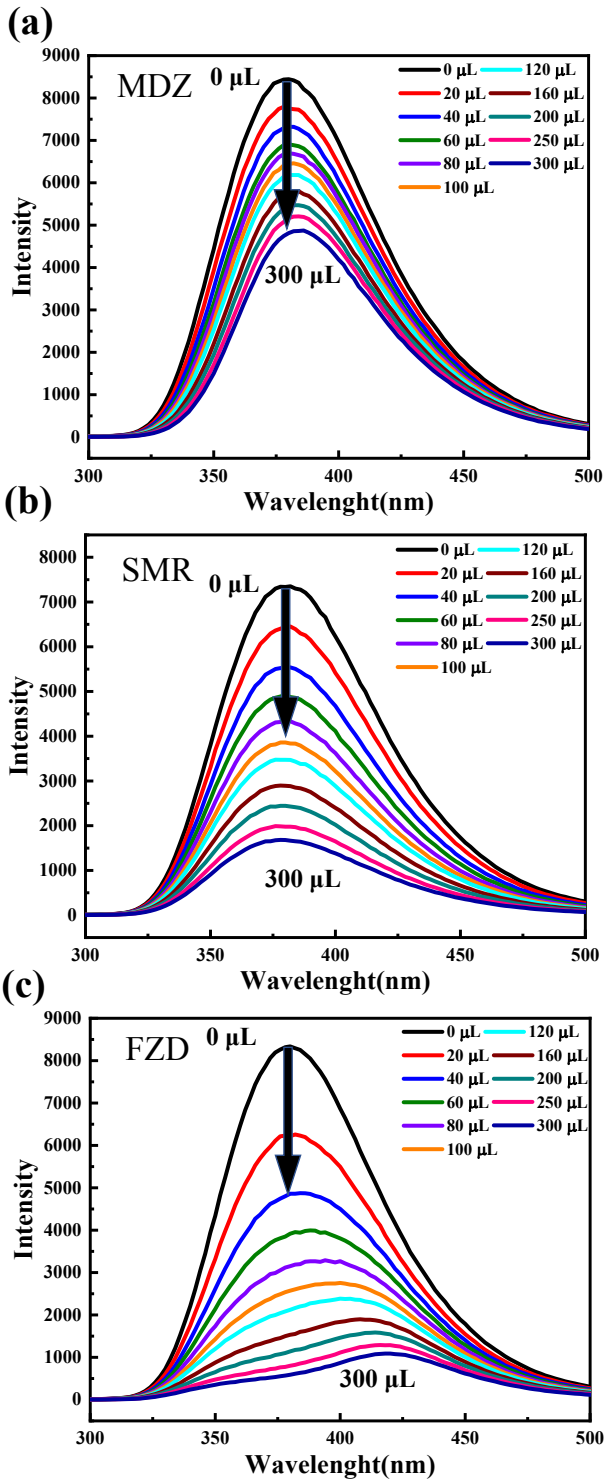


**Fig. S20** The change of the fluorescence of aqueous **BUT-172** suspensions upon the incremental addition of 300 µL aqueous solution of (a) MDZ, (b) SMR, and (c) FZD (500 µM).

Table S1. HOMO and LUMO energies calculated for selected anlytes used at B3LYP/6-31G*level.

| Analytes | HOMO (ev) | LUMO (ev) | Band Gap (ev) |
|---|---|---|---|
| KAN | -5.473 | 1.345 | 6.818 |
| APR | -5.176 | 1.139 | 6.315 |
| ERY | -5.472 | -0.636 | 4.836 |
| STR | -5.854 | -1.325 | 4.529 |
| PCL | -5.558 | -1.777 | 3.781 |
| ENR | -6.264 | -1.837 | 4.427 |
| CIP | -6.274 | -1.841 | 4.433 |
| NOR | -6.450 | -2.020 | 4.430 |
| THI | -6.206 | -2.661 | 3.545 |

Table S2. Crystal data and structure refinement for **BUT-172** and **BUT-173**.

| | **BUT-172** | **BUT-173** |
|---|---|---|
| Empirical formula | $C_{60}H_{45}In_3O_{15}$ | $C_{60}H_{45}In_3O_{15}$ |
| Formula weight | 1350.42 | 1350.42 |
| Measurement temperature | 293(2) K | 293(2) K |
| Crystal system | Orthorhombic | Monoclinic |
| Space group | *Pnma* | $P2_1/n$ |
| *a* (Å) | 49.7021(5) | 18.9338(6) |
| *b* (Å) | 7.26820(10) | 29.1926(9) |
| *c* (Å) | 30.1678(4) | 20.8268(7) |
| *α* (°) | 90 | 90 |
| *β* (°) | 90 | 113.720(4) |
| *γ* (°) | 90 | 90 |
| Volume(Å$^3$) | 10898.0(2) | 10539.1(7) |
| Z | 4 | 4 |
| Calculated density(g cm$^{-3}$) | 0.823 | 0.687 |
| Absorption coefficient (mm$^{-1}$) | 5.321 | 1.847 |
| Independent reflections ($I > 2\sigma(I)$) | 11102 [$R$(int) = 0.0317] | 3860 [$R$(int) = 0.2153] |
| $F$(000) | 2688 | 2688 |
| Reflections collected | 34774 | 64310 |
| $\vartheta$ range for data collection | 3.847-70.496° | 3.365-26.372° |
| Data/restraints/parameters | 11102/0/412 | 21510/0/706 |
| Limiting indices | –53 ≤ $h$ ≤ 60 | –23 ≤ $h$ ≤ 18 |
| –33 ≤ $k$ ≤ 27 | –7 ≤ $k$ ≤ 8 | -34 ≤ $h$ ≤ 36 |
| –33 ≤ $l$ ≤ 33 | –35 ≤ $l$ ≤ 36 | -16 ≤ $h$ ≤ 26 |
| Goodness-of-fit on $F^2$ | 1.069 | 1.034 |
| $R_1$ [a], $wR_2$ [b] [$I > 2\sigma(I)$] | $R_1$ = 0.0475, $wR_2$ = 0.1314 | $R_1$ = 0.0491, $wR_2$ = 0.0968 |
| $R_1$ [a], $wR_2$ [b] (all data) | $R_1$ = 0.0613, $wR_2$ = 0.1416 | $R_1$ = 0.0759, $wR_2$ = 0.1080 |
| Largest diff. peak and hole (e/Å$^3$) | 0.988 and –1.070 | 2.021 and -0.976 |

[a] $R_1 = \sum||F_o| - |F_c||/\sum|F_o|$. [b] $wR_2 = [\sum w(F_o^2 - F_c^2)^2/\sum w(F_o^2)^2]^{1/2}$